

InterPACKICNMM2015-48375

EXPERIMENTAL CHARACTERIZATION OF THE TRANSIENT RESPONSE OF AIR/WATER CROSSFLOW HEAT EXCHANGERS FOR DATA CENTER COOLING SYSTEMS

Marcelo del Valle
Villanova University
Villanova, PA, USA

Alfonso Ortega
Villanova University
Villanova, PA, USA

ABSTRACT

Data Center hybrid air/liquid cooling systems such as rear door heat exchangers, overhead and in row cooling systems enable localized, on-demand cooling, or “smart cooling.” At the heart of all hybrid cooling systems is an air to liquid cross flow heat exchanger that regulates the amount of cooling delivered by the system by modulating the liquid or air flows and/or temperatures. Due the central role that the heat exchanger plays in the system response, understanding the transient response of the heat exchanger is crucial for the precise control of hybrid cooling system. This paper reports on the transient experimental characterization of heat exchangers used in data centers applications. An experimental rig designed to introduce controlled transient perturbations in temperature and flow on the inlet air and liquid flow streams of a 12 in. x 12 in. heat exchanger test core is discussed. The conditioned air is delivered to the test core by a suction wind tunnel with upstream air heaters and a frequency variable axial blower to allow the control of air flow rate and bulk temperature. The conditioned water is delivered to the test core by a water delivery system consisting of two separate water circuits, one delivering cold water, and the other hot water. By switching from one circuit to the other or mixing water from both circuits, the rig is capable of generating step, ramp and frequency perturbations in water temperature at constant flow or step, ramp or frequency perturbations in water flow at constant temperature or combinations of temperature and water flow perturbations. Experimental data are presented for a 12x12 heat exchanger core with a single liquid pass under different transient perturbations.

INTRODUCTION

Traditionally data centers are cooled using perimeter air cooling systems (Figure 1). The systems operate by providing cold air from a Computer Room Air Handler (CRAH) to a raised floor plenum which distributes the cold air and injects it

to the front of the server racks. The cold air is sucked into the racks by the server fans, cools the electronic components and then is expelled from the servers where it flows back to the CRAH unit where the heat is transferred to water via a cross flow heat exchanger. Centralized cooling systems such as this do not easily allow control of local thermal management in a single aisle, and certainly not to a single rack of servers. The amount of air injected to the raised floor is controlled by the CRAH units serving the room. No direct control exists in the amount of air that each server rack receives. When the amount of air provided by the cooling system to a specific rack is not sufficient to maintain the servers at a safe temperature, data centers operators typically increase the amount of cold air provided by the CRAH units, thus overprovisioning the entire room. Servers with large computing loads are maintained in a safe temperature range however servers with a small work load or in an idle state are overcooled. Since the load in the servers are controlled by workload schedulers that increasingly will attempt to maximize server utilization in time, the hot spots can appear and disappear or move around the room as workload is assigned. It is clear that centralized cooling systems are not suited for localized dynamic cooling that can be operated synergistically with workload allocators. To overcome these issues, distributed and dynamically controlled cooling systems are required. Hybrid air-liquid cooling systems that can be distributed within the data center room and deployed in closer proximity to racks/servers are one promising approach. Such systems provide local air-cooling to servers, but they absorb the heat and move it over the larger distances required to remove heat from the room by a liquid coolant. At the heart of all of these systems is the air-to-liquid heat exchanger that is the subject of the current investigation.

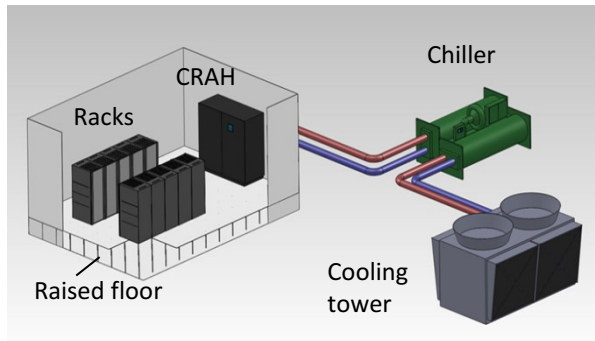


Figure 1. Data center perimeter cooling representation

Hybrid Air-Liquid cooling systems such as rear door heat exchanger systems (Figure 2a), In-row (2b), and overhead (2c) cooling systems provide an alternative to traditional perimeter cooling systems. In a Hybrid Cooling system, air is used to cool the CPUs, as in a normal air cooled system but the cooling systems are distributed such as to be “closely coupled” to the server racks. This approach avoids most of the mixing between cold and hot air present in a conventional air cooling systems and permits close control of the amount of cooling provided to each rack. At the heart of each of these systems is a cross-flow heat exchanger that controls system performance (Figure 2d). In true dynamic, close-coupled systems, the cooling system is operated dynamically and synergistically with the dynamic IT load allocation so as to provide local, on-demand cooling. In order to provide dynamic control to the hybrid cooling system, validated transient cross flow heat exchanger models are required. One of the biggest problems in validating a transient cross flow heat exchanger model is the absence of detailed experimental data in the literature. Most of the previous work [1-6] fails to present sufficient detail about the data thus making it difficult or impossible to use the data to validate a mathematical model. Others [7-9] present their results in the frequency space domain, again making it difficult to use the data in a code validation process. In general, it is possible to induce a transient response in a heat exchanger by introducing a time varying inlet temperature or mass flow rate on either the air side or the liquid side. In most of the cases only the transient perturbation in temperature using step functions has been studied. No detailed data exist for ramp or frequency changes in temperature and almost no data is available for changes in mass flow.

This paper will describe the development of an experimental apparatus for introducing a time varying temperature or mass flow at the inlet of the air side or the liquid side of a test heat exchanger core. The rig was designed to produce different types of perturbations (step, ramp, frequency) in flow or temperature independently or in combination, either in the liquid or air streams. Sample data from a single pass air-water cross-flow heat exchanger will be discussed.

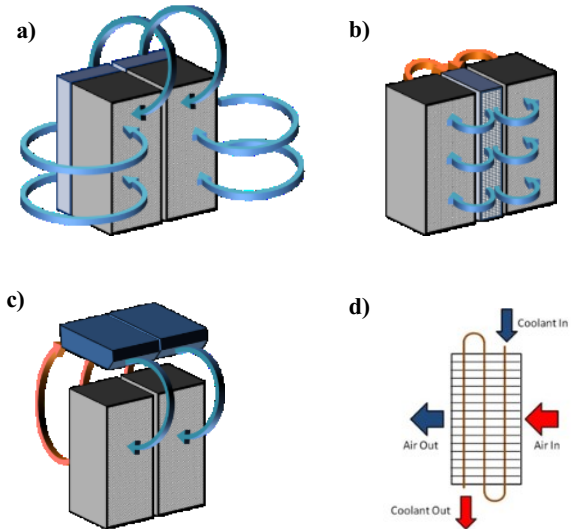


Figure 2. Hybrid cooling systems: a) Rear door heat exchanger, b) In Row cooling system, c) Over head cooling system, d) Cross flow heat exchanger In-row

NOMENCLATURE

t	time, s
m	mass, kg
T	Temperature, °C
f	Frequency, Hz
v	Voltage, V
r	Electric resistance, Ω
V	Volumetric flow, m^3/s
c	Specific heat, $\text{J/kg}\cdot\text{K}$

Greek symbols

ε	Effectiveness
ρ	Density, kg/m^3
ϕ	Phase angle

Subscripts

w	Water
a	Air
hx	Heat exchanger
al	Aluminum
cu	Copper

EXPERIMENTAL APPARATUS

The experimental set up was divided in two different sections to provide conditioned air and water flow respectively. The first section (Figure 3) consists of an open suction wind tunnel driven by an axial blower. Air is sucked into the wind tunnel air inlet and passed through a flow inlet section where a honeycomb screen and a set of tensioned mesh screens straighten the flow and dissipate large turbulent eddies present in the flow. Air then flows through the 6:1 contraction where it is accelerated, stretching the remnant vortex filaments present in the flow and thereby dissipating them [10]. The air exits into a mixing plenum and a 12x12 in test section that holds the test

heat exchanger core, Figure 4. Finally the flow exits into a diffuser which decelerates the flow entering the axial blower at the rearward part of the wind tunnel and expulsing the air to the room. The air speed is measured using a PDA-18-F-16-KL United Sensor Pitot tube directly after the contraction, where the air flow has a uniform profile. The difference between static and total pressure was measured using a 0-10[torr] Baratron™ differential pressure transducer while the static pressure was measured using a 0-2.5[inH2O] Setra™ pressure transducer. A 1/8in type-K thermocouple probe was inserted in the same section to measure the air inlet temperature. Two 1/8 in. static pressure probes were placed at the inlet and outlet of the heat exchanger to measure the static pressure drop. The differential pressure between the pressure probes was measured using a 0-10[inH2O] Setra™ differential pressure transducer. The outlet average temperature was measured using a thermocouple grid consisting of 25 30 AWG type K thermocouples distributed in 5 rows of 5 thermocouples each connected in parallel. The relation between the voltage generated by each thermocouple and the average voltage generated by the thermocouple grid has the following expression:

$$v_0 = \frac{\sum_{j=1}^n \frac{v_j}{r_j}}{\sum_{j=1}^n \frac{1}{r_j}} \quad (1)$$

Where r_i represents the resistance of each thermocouple wire. Special attention was taken to cut each thermocouple at the same size to keep the same resistance in each one.

A set of air heaters and a gate could be added in front of the test section to study changes in the air temperature or the influences of obstructions in the flow as desired.

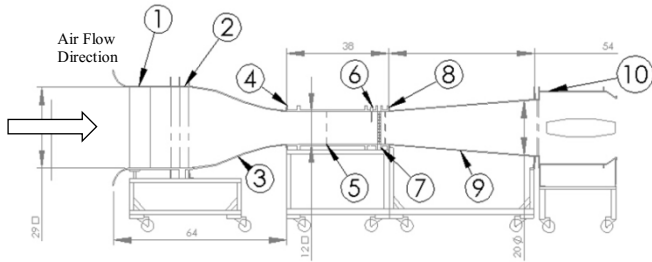


Figure 3. Suction wind tunnel. (1) air inlet, (2) inlet flow management section, (3) 6:1 contraction, (4) flow and temperature measurement, (5) mixing plenum, (6) static pressure measurement, (7) 12x12 air to water cross flow heat exchanger, (8) outlet air temperature and static pressure measurement, (9) diffuser, (10) axial blower

The second part of the experimental rig consisted of two 85 gallon pressurized water tanks and a signal generation section (Figure 5). The two tanks were operated at different temperatures, with one held at a higher temperature than the other. Step changes in temperature at constant flow were achieved by switching the water flow from one tank to the other using a 3/4in manual three way valve (Figure 5b). Ramp or periodic changes in water temperature were achieved by

replacing the three way manual valve with a 3/4in Tee and mixing water from both tanks using two Belimo™ G220s linear control valves with Belimo™ NKQX24-MFT actuators (Figure 5b). The water tanks were pressurized with compressed air from a common air pressure regulator which was connected to both tanks to guarantee equal pressure in both tanks. This characteristic was especially important for cases that required constant flow during the transient perturbation.

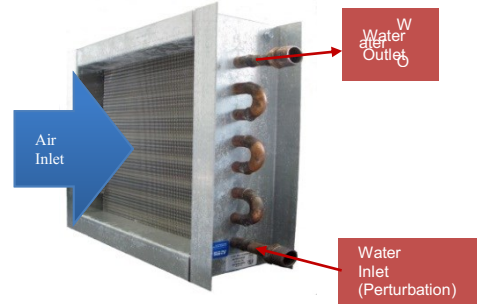


Figure 4. Tested heat exchanger core

Since the tanks were pressurized equally, the water flow remained constant after switching the three way valve or modulating the two linear control valves. One electronically controlled 3000W electric heater immersed in the water tank at its base raised the water temperature in each tank and kept it at the desire temperature. Submersible water pumps were placed inside the tanks and used to stir the water inside the tanks to guarantee uniform temperature. A 3/4in OMEGA™ FTB-371 turbine flow meter was chosen to measure the volumetric flow rate due its small time response. A Honeywell TJE 0-100psi wet pressure transducer was placed in the heat exchanger inlet to measure the total gauge pressure in the line. A Honeywell model Z 0-5psi wet differential pressure transducer with its ports placed in the heat exchanger inlet and outlet ports was used to measure the pressure drop during the experiments. Type K ungrounded 1/16 in. thermocouples probes were inserted inside the tanks and in the tank outlets. Type K exposed 1/16 in. thermocouples probes were used in the heat exchanger ports to measure the heat exchanger time response in the water side.

Heat exchanger Characteristic	Dimension
Pipe OD	5/8 in
Fins per inch	10
Fins type	Flat
Number of circuits	1
Number of pipes	8
Dimensions H x W x D	12x12x5 in
Fins material	Aluminum
Tube material	Copper
Heat exchanger thermal capacitance ($m_{hx} \cdot c_{hx}$)	1348 J/K
Heat exchanger core mass (m_{hx})	1.81 kg

Table 1. Heat exchanger characteristics

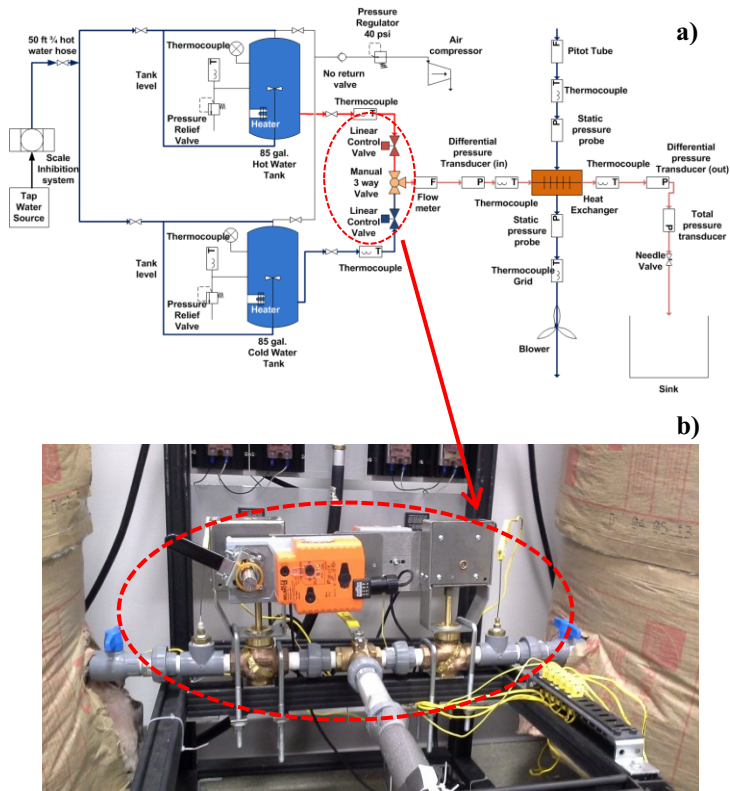


Figure 5. Water tanks and water delivery system. a) System schematic, b) Signal generator section

All of the instrumentation was connected to a National Instruments cDAQ-9172 DAQ System and controlled using Labview™. Two NI9211 cards were used to measure the voltages signals generated by the thermocouples placed on the heat exchanger inlets and outlets while the rest of the thermocouples including the ice bath, were read by a NI9213 card. An additional NI9211 card was used to measure the low voltages signals provided by the two wet pressure transducers located in the heat exchanger water side. One NI9207 card was used to measure the signal provided by the dry pressure transducers. A NI9401 digital card was used to measure the pulses from the flow meter. The conversion to flow readings was performed in Labview™. Finally a NI9263 analog output card provided the 2-10V signal required to control the two linear control valves. The DAQ system configured in this way was capable of reading the signals and controlling the valves at a rate of 0.2 seconds.

The initial test sample was a 12x12 one pass cross flow heat exchanger (Figure 4). The heat exchanger characteristics are listed on Table 1. The heat exchanger copper tubing mass was estimated to be 0.56kg while the total fin mass was estimated to be 1.25 kg. The heat exchanger lumped specific heat (c_{hx}) was calculated as the summation of each component specific heat (copper pipes and aluminum fins) multiplied by the ratio of the component weight and the overall heat exchanger mass. The total heat exchanger thermal capacitance was calculated by multiplying the heat exchanger specific heat by the overall heat exchanger mass.

RESULTS AND DISCUSSION

Six cases using different perturbations in the water inlet condition are presented. The first three cases are for water temperature changes at constant water flow rate whereas the last three are related to water flow rate perturbation at constant temperature.

Step change in temperature at constant flow

Step changes in water temperature at constant flow were produced by switching the water tank feeding the heat exchanger using the 3 way manual valve. The valve switching time was approximately 0.5 seconds. Both linear control valves were in an open position during this operation. To initiate the experiment from steady state conditions, cold water was run through the system for 4 minutes. At $t=4$ minutes the 3 way manual valve was switched, allowing hot water flow through the heat exchanger and producing a near step-change in inlet water temperature. Hot water was allowed to flow through the heat exchanger for 4 minutes which was sufficient to allow the heat exchanger to achieve its new steady state. This procedure was repeated 8 times and the results were ensemble-averaged at each time step. To estimate the random error in the measurements the standard deviation of the 8 measurements in each time step were calculated. The synchronization between the different cases was performed manually by finding the moment when the first change in water temperature was read by the thermocouple placed in the heat exchanger inlet port. Since the heat transfer process is dominated by the difference in temperature between the two streams, the results of course would be non-dimensionally the same for cases with both a temperature increase and decrease in the inlet water temperature. Cases using different air and water flow were tested.

Figure 6 shows two of these cases. The figures show the temperature and flow measurements for each case. In case (a), the water flow rate was $1.3 \times 10^{-4} \text{ m}^3/\text{s}$ (2gpm) and an inlet temperature of 19.4°C . At the same time the air flow rate was $0.18 \text{ m}^3/\text{s}$ at 23.4°C . At $t=10\text{s}$ the temperature perturbation was introduced and water at 50.5°C was circulated through the heat exchanger at the same flow rate. A time delay of 2.2s and 4.4s was found in the air and water outlet temperatures. In the case of the water signal this effect is related mostly to the transit time of the water flowing in the heat exchanger pipe. The air outlet signal reaches 63.2% of its final steady state temperature 9.2s after the water temperature perturbation is introduced in the heat exchanger (one time constant). For the water outlet signal the time constant is 8.4s. The steady state effectiveness in this case was $\epsilon = 0.28$. For case (b), water flow rate was kept at $1.3 \times 10^{-4} \text{ m}^3/\text{s}$ (2gpm) and 19.7°C . The air flow was increased to $1.2 \text{ m}^3/\text{s}$ and kept at 23°C . Again the hot water perturbation was applied at $t=10\text{s}$ increasing the water temperature to 50.3°C . For this case the delays in the air and temperature outlet signal were 1.8s and 4.6s, very close to the delays observed in the previous case. Time constants for the air and

water outlet signals were found to be 7.2s and 7.8s, both smaller than the previous case.

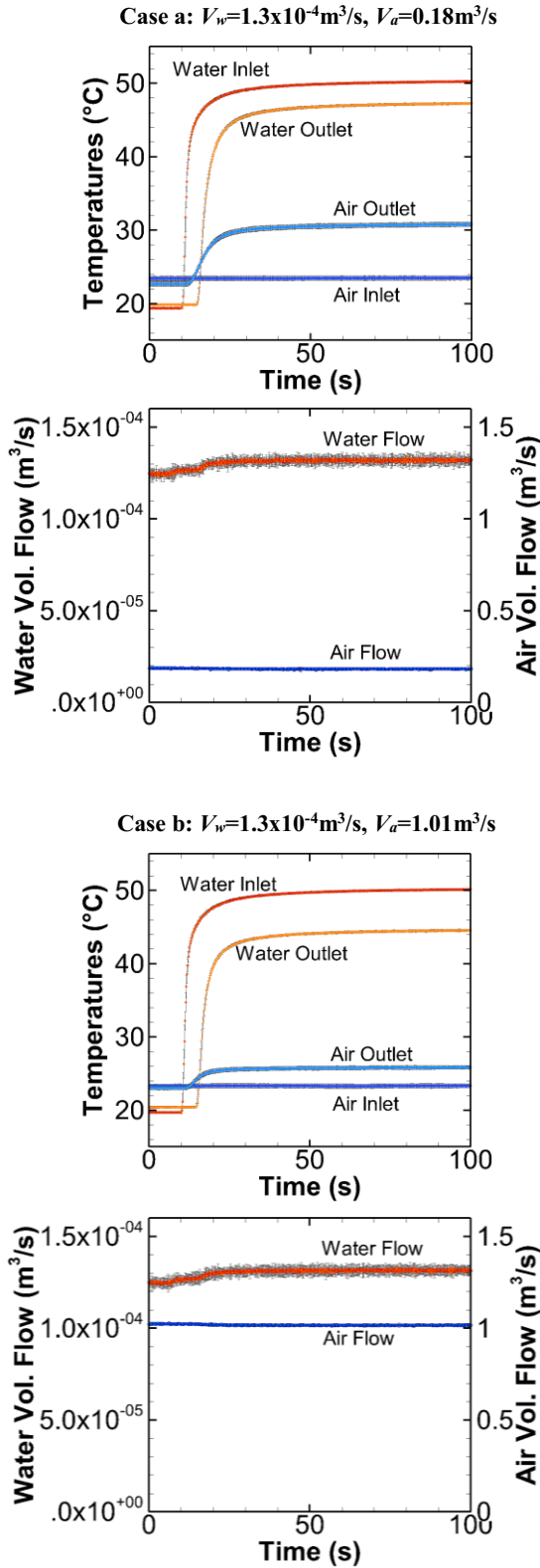


Figure 6. Cases for step change in temperature at constant flow

Error bars are shown for both cases. Before and after the perturbation was introduced, the fluctuations in the instantaneous water and air temperature measurements were on the order of 0.1°C and 0.3°C . During the small interval in which the manual step change was introduced, these fluctuations increased drastically (2°C in the water inlet signal and 1.1°C in the water outlet signal). The reason for this particular behavior can be found in the use of the manual valve to produce the perturbation. The use of a manual valve makes it impossible to exactly synchronize the different data sets during the averaging process. The use of a 3 way automatic valve would increase the experiment repeatability by using a single clock to control the signal generation and the data acquisition. Air signals during this period present errors of 0.3°C . Flow measurements show variations on the order of 4% for the water flow measurements and 4.1% for the air flow measurements. The difference in water volumetric flow before and after the perturbation was on the order of 5%. This minor change in water flow rate is attributed to minor differences in the experiment hydraulic resistance between the cold and hot water delivery sections and differences in the tank water levels.

Ramp change in temperature at constant flow

Ramp changes in water temperature at constant flow were produced by slowly closing the linear control valve placed in front of the cold tank and opening the linear control valve in front of the hot tank at the same rate. The manual three way valve was replaced by a $\frac{3}{4}$ CPVC tee to permit mixing between both streams. The 2-10V signal required to control the valves was generated using a NI9263 card controlled with LabviewTM. In order to start the experiment from steady state conditions, cold water was run through the system for 4 minutes. At $t=4$ minutes the ramp signal initiated, closing the cold water valve and opening the hot water valve in the same proportion. The process took 60 seconds. After the hot water valve achieved its full open position, hot water was flowed through the heat exchanger for another 3 minutes in order to reach steady state. This procedure was repeated 8 times and the results averaged in each time step. Again, the synchronization between the different cases was performed manually by finding the moment when the first change in water temperature is read by the thermocouple placed in the heat exchanger entrance. Cases using different air and water flow conditions were tested. Figure 7 shows two of these cases. Case (a) was performed by flowing water at $6.6 \times 10^{-5} \text{ m}^3/\text{s}$ and 21.1°C and increasing the water temperature to 50.1°C after the ramp was completed. Air flow rate was $0.27 \text{ m}^3/\text{s}$ at 23.7°C . Again delays in the air and water outlet signal were found. For the air signal the delay was estimated to be 6s and for the water stream the delay was 8s. The steady state effectiveness for this case was $\epsilon = 0.23$. In the second case water flow was increased to $1.3 \times 10^{-4} \text{ m}^3/\text{s}$ keeping the rest of the conditions constant (Air flow= 0.27 , Air temperature= 22.8°C , water temperature before perturbation= 22.3°C and 50.2°C after perturbation). This change produced a reduction in the delay time for the water outlet signal (4.6s)

compared with the first case but close to the results obtained for the step change case at the same water flow.

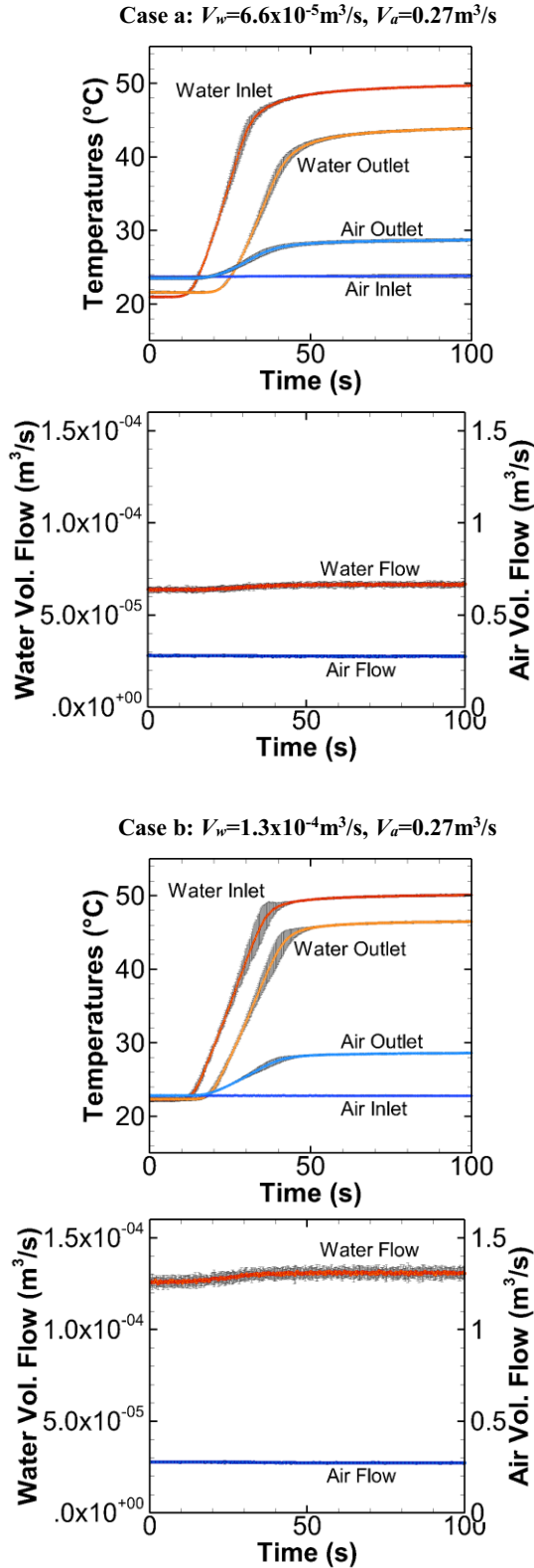


Figure 7. Cases for ramp change in temperature at constant flow

Errors were similar to the previous case. Maximum temperatures errors were on the order of 0.3 and 0.1°C for water and air measurements before and after the perturbation. Again they increased drastically when the perturbation was introduced, reaching 2°C close to the end for the water inlet signal. Flow measurements showed variations on the order of the 4% for the water flow measurements and 4% for the air flow measurements. The difference in water volumetric flow before and after the introduction of the perturbation was 3.5%.

Frequency change in temperature at constant flow

Frequency changes in water temperature at constant flow were produced by mixing hot and cold water in a periodic fashion. By opening one linear control valve and closing the other linear control in the same proportion constant water flow was guaranteed. The manual three way valve was replaced by a $\frac{3}{4}$ CPVC Tee to allow mixing between both streams. Again the control valves were controlled using Labview™ and a NI9263 card which sent triangular voltage signals between 2-10V to the valves controlling their movements. The system was run until a periodic state was reached. Ten cycles were recorded and phase averaged. Cases using different flow rates in air and water and different frequencies were tested.

Figure 8 shows two of these cases. In case (a), water was flowed through the system at $6.6 \times 10^{-5} \text{ m}^3/\text{s}$. The sinusoidal temperature signal had a maximum of 44.2°C and a minimum of 25.4°C. Air flow rate through the heat exchanger was $0.37 \text{ m}^3/\text{s}$ at 23.3°C. Under these conditions the outlet water signal demonstrated a phase shift of -180° with respect to the water inlet signal. Also the signal was attenuated in amplitude with respect to the inlet water signal, having a maximum of 37.2°C and a minimum of 26.4°C. The air outlet signal presented a similar behavior. The phase shift between the air outlet signal and the water inlet signal was -93.6° and the maximum and minimum values were 25.8° and 24.3°C. In the second case water flow was increased to $1.25 \text{ m}^3/\text{s}$. The measured maximum and minimum inlet temperatures were 46.4°C and 23.8°C respectively. Air inlet condition were kept at $0.37 \text{ m}^3/\text{s}$ at 23.4°C. The change in water flow conditions produced a change in the phase shift in both outlet signals with respect to the inlet water signal. The phase shift for the water outlet signal was calculated to be -93.6° and the air outlet signal was phase shifted by 68.4° . As in the first case the water and air temperature outlet signals were attenuated with respect to the inlet perturbation. For the water outlet signal the maximum and minimum temperatures were 41.9°C and 25°C and for the air outlet signals these values were 26.9°C and 24.2°C. Maximum temperatures fluctuations were on the order of 0.5°C and 0.1°C for water and air measurements respectively. Water flow measurements showed variations on the order of the 2.6%, whereas air flow measurements showed variations of 1.7% of the reading.

Case a: $V_w=6.6 \times 10^{-5} \text{ m}^3/\text{s}$, $V_a=0.27 \text{ m}^3/\text{s}$, $f=0.05 \text{ Hz}$

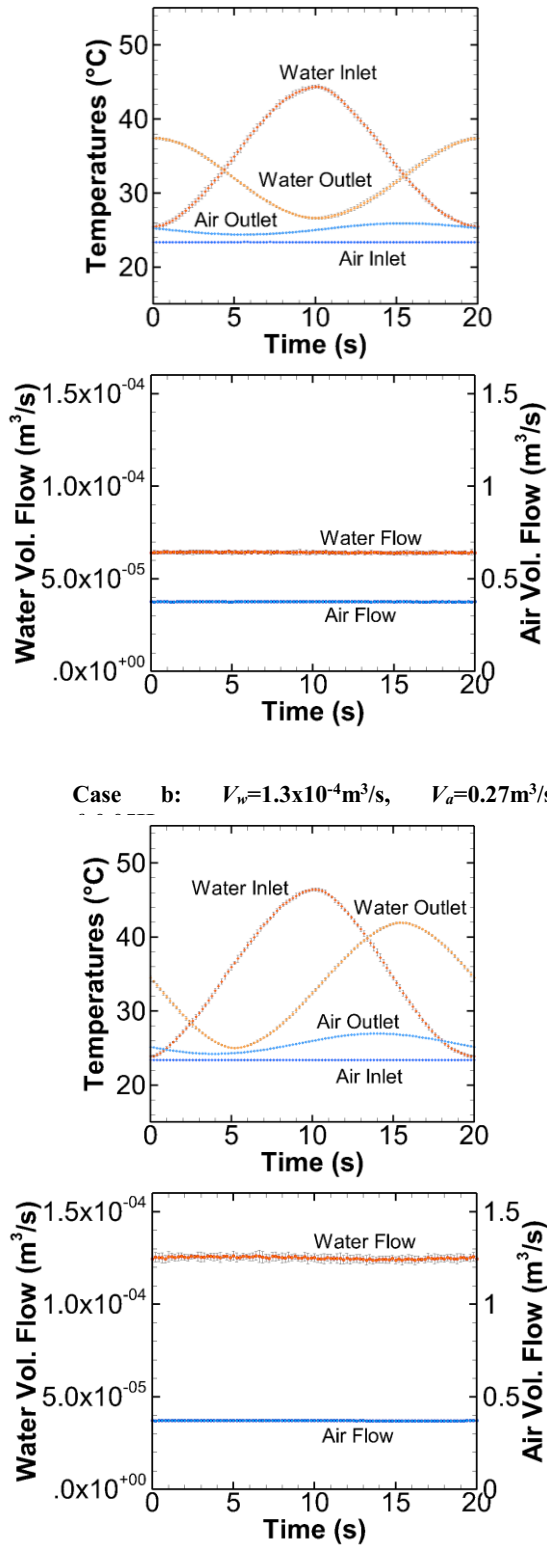


Figure 8. Cases for frequency change in temperature at constant flow

In case (a), water was flowed through the system at $6.6 \times 10^{-5} \text{ m}^3/\text{s}$. The sinusoidal temperature signal had a

Step change in flow at constant temperature

To produce step changes in water flow at constant temperature only the hot water tank was used. The valves in the cold tank were closed to avoid mixing between the tanks. The butterfly valve placed on the heat exchanger outlet had a settable intermediate position between the totally closed and totally open positions. To start the experiment, the valve was kept in the intermediate position. Hot water was flowed through the heat exchanger until the system reached steady state. After steady state was reached the valve was totally opened allowing an increase in the water flow. This procedure was repeated 8 times and the results averaged in each time step. The synchronization between the different cases was performed manually by finding the first change in water flow read by the flow meter. Cases using different air flow rates were tested. Figure 9 shows one of these cases.

Case: $V_w=1.3 \times 10^{-4} - 3.1 \times 10^{-4} \text{ m}^3/\text{s}$, $V_a=0.28 \text{ m}^3/\text{s}$

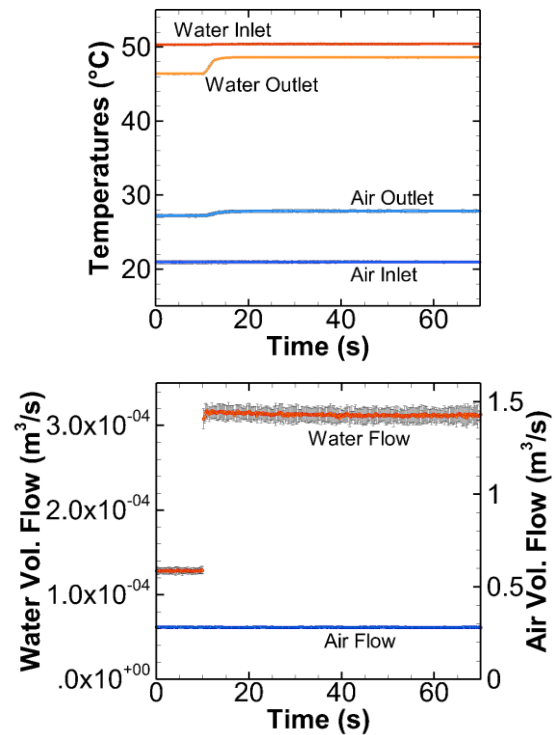


Figure 9. Step change in flow at constant temperature

Hot water at 50.3°C was circulated through the heat exchanger at $1.3 \times 10^{-4} \text{ m}^3/\text{s}$ (2gpm). At $t=10\text{s}$ the water flow was increased to $3.1 \times 10^{-4} \text{ m}^3/\text{s}$ (5gpm) and kept there until steady state was reached. At $t=10.4\text{s}$ the water outlet signal started to raise, going from 46.8°C to 48.6°C in 6.4s . Similar changes were produced in the air outlet stream where the temperature start to increase from 27.2°C at $t=10.6\text{s}$ to 27.9°C at $t=17\text{s}$. The system time response was short compared with the step temperature changes at constant flow cases. Two competing effects, the convection between the water and inside pipe wall and advection in the water flow, were observed in the water outlet temperature results. Even when the heat transfer

coefficient inside the pipe rose due to the increase in water flow, the outlet water temperature signal increased due to the advective effects of higher water velocities.

Maximum temperatures fluctuations were found to be on the order of 0.2°C for all measurements. Water flow measurements showed variations on the order of the 4% of the reading while air flow measurements showed a variation of 2.7%.

Ramp change in flow at constant temperature

Ramp changes in flow were produced using the linear control valve placed in the water hot tank outlet. The valves in the cold tank were closed to avoid any kind of mixing with cold water. The linear control valve was partially closed and water flowed through the heat exchanger until the system reached steady state. Once steady state was reached the valve was slowly opened increasing the hot water flow rate. After the flow reached its maximum value, water was flowed through the heat exchanger for one minute. This procedure was repeated 8 times and the results averaged in each time step. The synchronization between the different cases was performed manually by finding the first change in water flow read by the flow meter. Cases using different air flow were tested. Figure 10 shows one of these cases.

Case: $V_w=7.7 \times 10^{-5} - 2.7 \times 10^{-4} \text{ m}^3/\text{s}$, $V_a=0.28 \text{ m}^3/\text{s}$

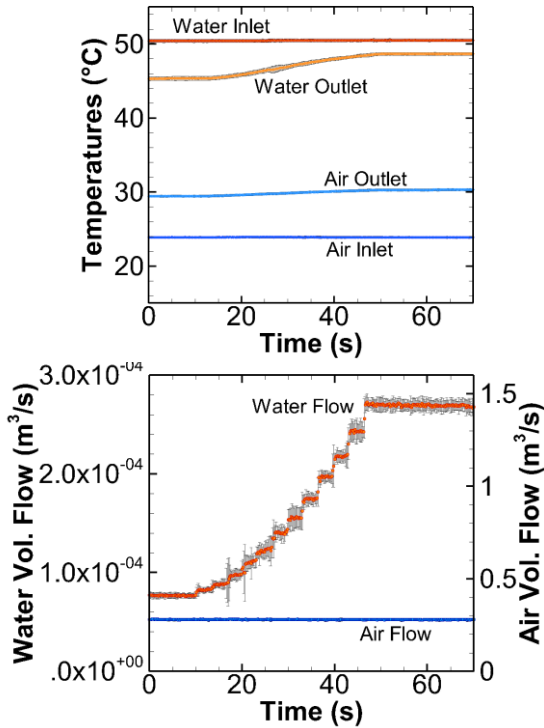


Figure 10. Ramp change in flow at constant temperature

Air was circulated through the heat exchanger at a rate of $0.28 \text{ m}^3/\text{s}$ and 23.9°C . At the same time hot water was circulated through the system at $7.7 \times 10^{-5} \text{ m}^3/\text{s}$ and 50.4°C . Under this condition air and water outlet temperatures were 29.4°C and 45.3°C respectively. At $t=10\text{s}$ a 36.6s flow ramp was

introduced, raising the water flow to $2.7 \times 10^{-4} \text{ m}^3/\text{s}$ and keeping the water temperature constant. The ramp change shows discrete rather than continuous changes in flow due to the valve actuator resolution. This change in flow produced a ramp increase in the outlet air and water temperatures raising their values to 30.3°C and 48.7°C respectively. Water outlet temperature started to rise at $t=13.2\text{s}$ (3.2 seconds after the flow ramp was introduced) and reached steady state at 51.2s . The air outlet signal also started to rise at $t=13.2$ seconds, reaching steady state at $t=72\text{s}$. The maximum temperature measurement fluctuations were on the order of 0.24°C and 0.5°C for the water inlet and outlet signals. On the other hand, air temperature measurements had errors on the order of 0.2°C . Water flow measurements show variations on the order of the 4% and air flow measurements are 1.2%.

Periodic change in flow at constant temperature

Periodic changes in flow were introduced by cyclically opening and closing the linear control valve placed in front of the hot tank with periodic square wave inputs. The valves in the cold tank were closed to avoid any kind of mixing with cold water. The system was run until a periodic state was achieved, at which time data was recorded. Ten cycles were recorded and phase averaged. Cases using different flow rates in air and water and different frequencies were tested. Figure 11 shows one of these cases.

Case: $V_w=7.4 \times 10^{-5} - 3.1 \times 10^{-4} \text{ m}^3/\text{s}$, $V_a=0.27 \text{ m}^3/\text{s}$, $f=0.1\text{Hz}$

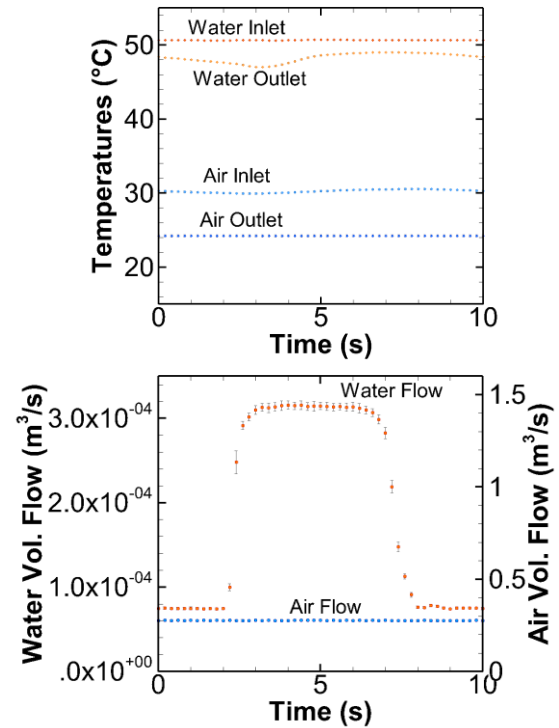


Figure 11. Frequency perturbation in flow at constant temperature

Air was circulated through the heat exchanger at a rate of $0.27 \text{ m}^3/\text{s}$ and 24.1°C . Hot water at 50.6°C was circulated

through the system at $7.4 \times 10^{-5} \text{ m}^3/\text{s}$ for 2 seconds, then increased to $3.1 \times 10^{-4} \text{ m}^3/\text{s}$ for 5 seconds and reduced again to $7.4 \times 10^{-5} \text{ m}^3/\text{s}$ for another 2 seconds. As expected, the rise in water flow produced an increment in the outlet air and water temperatures and the reduction in water flow was followed by a drop in those temperatures. Even when the water flow signal is symmetrical, the outlet temperature signals are not. The air outlet temperature signal presents a maximum value of 30.6°C at $t=7.8\text{s}$ and a minimum of 30.0°C at $t=3\text{s}$ meanwhile the water outlet temperature signal showed a maximum value of 49.0°C at $t=7\text{s}$ and a minimum of 47.0°C at $t=3.2\text{s}$.

Maximum temperature fluctuations were on the order of 0.1°C for all the temperature measurements. Water flow measurements showed variations on the order of the 1.7% of the reading meanwhile air flow measurements were 1.3% of the reading.

CONCLUSIONS

Prior work has documented experimental result for cross flow heat exchanger under transient temperature perturbations. However most of the available data is related to step changes in temperature at constant flow and almost no data is available for other types of perturbations in temperature or flow. In this study we designed, built and tested an experimental facility to perform transient experiments on 12x12in cross flow heat exchangers under transient temperature and flow perturbations. Results under step changes in temperature showed similar behavior as those presented by Ataer [1] and Ataer and Gou [2] where the outlet temperature signals presented a time delay with respect to the inlet temperature perturbation. This delay is related to the time that water takes to travel inside the heat exchanger pipes. Furthermore, it was found that under sinusoidal temperature perturbations, the water flow rate controls the phase shift angle between the temperature signal perturbation (inlet temperature signal) and the two temperatures signal responses (outlet air and water temperatures).

Cases using different air flow rates showed the dependence of the outlet temperature signals with the air flow rate.

Flow change scenarios showed shorter system reaction times and almost no delay between the application of the water flow perturbation and the temperature responses. Two competing effects, the convection between the water and inside pipe wall and advection in the water flow, were observed in the water outlet temperature results. Even when the heat transfer coefficient inside the pipe rises due the increase in water flow, the outlet water temperature signal increased due to the advective effects produced by the higher water velocities.

Future work using detailed validated heat exchanger models will extend the discussion over the transient response of heat exchangers under flow and temperature perturbations.

ACKNOWLEDGEMENTS

This material is based upon work supported by the National Science Foundation Center for Energy Smart Electronic

Systems (ES2) under Grant No. IIP-1134810. Any opinions, findings, and conclusions or recommendations expressed in this material are those of the author(s) and do not necessarily reflect the views of the National Science Foundation.

REFERENCES

- [1] Ataer, Ö.E., An approximate method for transient behavior of finned-tube cross-flow heat exchangers. *International journal of refrigeration*, 2004. 27(5): p. 529-539.
- [2] Ataer, Ö.E., A. İleri, and Y. Göğüş, Transient behaviour of finned-tube cross-flow heat exchangers. *International journal of refrigeration*, 1995. 18(3): p. 153-160.
- [3] Díaz, G., et al., Dynamic prediction and control of heat exchangers using artificial neural networks. *International journal of heat and mass transfer*, 2001. 44(9): p. 1671-1679.
- [4] Gogus, Y. and O. Ataer, Effect of fins on transient behavior of cross-flow air-liquid heat exchangers, in *International Refrigeration and Air Conditioning Conference* 1988.
- [5] Yao, Y., Z. Lian, and Z. Hou, Thermal analysis of cooling coils based on a dynamic model. *Applied thermal engineering*, 2004. 24(7): p. 1037-1050.
- [6] Yao, Y. and S. Liu, The transfer function model for dynamic response of wet cooling coils. *Energy conversion and management*, 2008. 49(12): p. 3612-3621.
- [7] Gartner, J. and L. Daane, Dynamic response relations for a serpentine cross-flow heat exchanger with water velocity disturbance. *ASHRAE JOURNAL*, 1969. 11: p. 53-68.
- [8] Gartner, J.R., Simplified dynamic response relations for finned-coil heat exchanger. *ASHRAE Trans*, 1972. 78(Part 2): p. 163-169.
- [9] Tamm, H. and G. Green, Experimental multi-row crossflow heat exchanger dynamics. *ASHRAE Trans*, 1973. 79(Part 2): p. 9-18.
- [10] Cattafesta, L., C. Bahr, and J. Mathew, *Fundamentals of Wind-Tunnel Design. Encyclopedia of Aerospace Engineering*, 2010.